International Journal of Future Engineering Innovations

# Flood Susceptibility Assessment in the Anambra River Watershed Using the LOPCOW Weighting Technique

**Okafor OC [1*], Ono MN [2], Emengini EJ [3], Igbokwe OI [4]**
[14] Department of Surveying and Geoinformatics, Nnamdi Azikiwe University Awka, Anambra State, Nigeria

* Corresponding Author: **Okafor OC**

## Article Info

**ISSN (online):** 3049-1215
**Volume:** 03
**Issue:** 06
**Received:** 04-09-2026
**Accepted:** 05-10-2026
**Published:** 03-11-2026
**Page No:** 65-75

**Abstract**
Flood susceptibility in the Anambra River watershed was mapped by integrating eight conditioning factors—elevation, slope, height above nearest drainage (HAND), distance to major rivers, drainage density, topographic wetness index (TWI), rainfall, and soil clay content—with the logarithmic percentage change-driven objective weighting (LOPCOW) method. The factors were harmonized to a 30 m WGS 84 / UTM Zone 32N grid and evaluated over 2,010,837 complete-factor cells covering 1,809.7533 km². The LOPCOW weights were highest for slope (20.23%), HAND (16.79%), and elevation (14.29%), followed by river distance (12.28%), clay (11.71%), TWI (10.85%), rainfall (10.41%), and drainage density (3.45%). The weighted index ranged from 0.298647 to 0.890720. Five equal-width classes placed 1.3887 km² in very low, 16.2252 km² in low, 173.8287 km² in moderate, 974.1528 km² in high, and 644.1579 km² in very high susceptibility. High and very high classes together occupy 1,618.3107 km², or 89.42% of the mapped area. The highest class is concentrated in lower terrain close to drainage, with mean elevation of 27.596 m, HAND of 2.802 m, slope of 0.959°, and river distance of 844.742 m. Ward-level summaries identify Abegbu / Iyiora, Enugu-Otu, and Omasi as the portions with the largest high-plus-very-high areas. The resulting maps and tables provide a spatially explicit basis for prioritizing floodplain planning and local drainage assessment in the watershed.

**Keywords:** Anambra River, flood susceptibility, LOPCOW, geographic information systems, HAND, topographic wetness index, ward-level mapping, objective weighting

## 1. Introduction

Flooding is among the most consequential environmental hazards because it affects settlements, infrastructure, agriculture, and public services across river basins and rapidly growing urban areas. Flood susceptibility mapping translates terrain, hydrological, climatic, and soil characteristics into spatial information that can support land-use planning and disaster preparedness. Geographic information systems (GIS) and remote sensing enable these factors to be processed on a common grid and interpreted together, while multicriteria decision analysis provides a transparent framework for combining variables measured on different scales (Malczewski, 2006; Kazakis *et al*., 2015; Islam *et al*., 2025) [13, 14, 16]. Recent reviews describe an expanding range of GIS, remote-sensing, machine-learning, and hybrid approaches, with increasing attention to factor selection, spatial scale, and interpretability (Sen & Das, 2026) [22].

Nigeria's riverine and urban landscapes experience recurrent flooding under the combined influence of intense rainfall, low-lying terrain, channel proximity, drainage conditions, soil properties, and land-use change. In southeastern Nigeria, Anambra State includes both elevated terrain and broad lowland areas connected to the Anambra River and the lower Niger system. Local studies have applied GIS-based multicriteria methods to flood susceptibility in northern Anambra and Ayamelum, demonstrating the value of spatially explicit assessment for the state (Igboanugo *et al*., 2023; Okeke & Ekemezie, 2026) [11, 19]. Research in the

lower Niger basin around Onitsha likewise documents flood susceptibility as a regional planning concern (Chinedu *et al*., 2024) [3].

The physical controls represented in this study describe complementary parts of flood generation and accumulation. Elevation and HAND distinguish low-lying terrain from higher ground and express relative height above drainage pathways. Slope influences runoff velocity and the opportunity for surface water to accumulate. TWI represents the tendency for topographic convergence and soil wetness, while distance to major rivers indicates proximity to channel overflow corridors. These terrain and drainage indicators are widely used in index-based flood mapping because they represent the spatial structure of surface flow and storage (Beven & Kirkby, 1979; Nobre *et al*., 2011; Sørensen *et al*., 2006; Kazakis *et al*., 2015) [2, 14, 18, 23].

Rainfall supplies water to the drainage system, drainage density describes the concentration of channel pathways, and soil clay content provides information about texture-related infiltration behavior. Their combined spatial pattern can differentiate areas where rainfall input meets low relief, limited drainage capacity, and near-channel position. The eight-factor design therefore combines terrain, channel proximity, drainage structure, wetness, rainfall, and soil texture in a single spatial assessment. Comparable Nigerian studies have used related combinations of terrain and hydroclimatic indicators, while recent national and international work continues to expand the range of data-driven and GIS-based approaches (Chinedu *et al*., 2024; Islam *et al*., 2025; Montien Tique *et al*., 2026; Isioye *et al*., 2026) [3, 12, 13, 17].

A multicriteria model requires each factor to be normalized to a common scale and assigned a weight before the normalized layers are combined. Expert-based methods such as the analytic hierarchy process are common in flood mapping, while objective methods derive weights from the distributions of the input criteria. LOPCOW uses the relationship between normalized root-mean-square values and standard deviations to calculate criterion weights and has been applied as a distribution-driven weighting procedure in multicriteria assessment (Ecer & Pamucar, 2022) [5]. Its use here makes the weighting calculation reproducible from the raster-cell matrix and allows the relative influence of each factor to be reported alongside the susceptibility classes.

Despite the growth of GIS-based and data-driven flood studies in Nigeria, a watershed-focused assessment that combines the eight specified terrain, drainage, rainfall, and soil factors with LOPCOW provides a useful spatial contribution for the Anambra River corridor. The analysis links factor distributions, objective weights, continuous index values, five susceptibility classes, and ward-level summaries. This integrated presentation makes the spatial pattern and its relationship to the selected criteria clear for watershed planning and prioritization.

This study assesses flood susceptibility in the Anambra River watershed using eight conditioning factors and the LOPCOW objective-weighting method. The objectives are to describe the spatial distributions of the factors, calculate their LOPCOW weights, generate and classify a continuous susceptibility index, and summarize susceptibility by watershed-clipped ward portions.

## 2. Materials and Methods

### 2.1. Study Area

Anambra State is located in southeastern Nigeria on the eastern plains of the River Niger. Its landscape includes rolling lowlands, riverine plains, and localized hills, while the humid tropical climate supports a marked rainy season and substantial surface-water input. The Anambra River, also known as the Ọmambala, is a major tributary of the Niger and provides the principal drainage corridor relevant to this assessment (Anambra State Government, n.d.; Igboanugo *et al*., 2023) [11].

The study focuses on the Anambra River watershed in Anambra State, where low-lying riparian plains meet gently rolling uplands. The watershed forms part of the lower Niger drainage system, making local relief, river proximity, and drainage pathways central to flood susceptibility (Anambra State Government, 2026; Chinedu *et al*., 2024; Igboanugo *et al*., 2023) [1, 3, 11].

### 2.2. Data Inventory and Provenance

The analysis used eight single-band GeoTIFF factor rasters, a watershed polygon, and GRID3 ward polygons for spatial summarization (GRID3, n.d.). Table 1 lists the source attribution and spatial support of the datasets, while Table 2 records the original raster grids, cell sizes, data types, extents, and NoData values.

**Table 1:** Spatial datasets and source attribution

| Dataset / format | Source attribution | Native source support |
|---|---|---|
| Elevation / GeoTIFF | SRTM elevation; USGS EarthExplorer | Approximately 30 m |
| Slope / GeoTIFF | SRTM-derived terrain gradient | Approximately 30 m |
| HAND / GeoTIFF | Terrain and drainage-network factor | 30 m |
| River distance / GeoTIFF | HydroSHEDS river network | Hydrographic network |
| Drainage density / GeoTIFF | HydroSHEDS drainage network | Hydrographic network |
| TWI / GeoTIFF | DEM-derived wetness factor | Terrain support |
| Rainfall / GeoTIFF | CHIRPS rainfall product | 0.05° native grid |
| Clay / GeoTIFF | ISRIC SoilGrids clay layer | 250 m native grid |
| Wards / ESRI shapefile | GRID3 operational wards | Vector polygons |
| Basin boundary / ESRI shapefile | Anambra River watershed polygon | Vector polygon |

Sources for the principal elevation, rainfall, soil, hydrography, and ward products are documented by Farr *et al.* (2007), U.S. Geological Survey (2018), Funk *et al*. (2015), Hengl *et al*. (2017), Poggio *et al*. (2021), Lehner *et al*. (2008), and GRID3 (n.d.).

The elevation layer represents SRTM terrain information, and the slope layer represents terrain gradient. The SRTM mission provides elevation measurements for regional-scale terrain analysis (Farr *et al*., 2007; U.S. Geological Survey, 2018) [6, 24].

Rainfall was represented by a CHIRPS-derived raster. CHIRPS combines satellite observations with station data to provide gridded rainfall estimates suitable for regional spatial analysis (Funk *et al*., 2015; Climate Hazards Center, n.d.) [7].

The clay layer represents SoilGrids soil-texture information. SoilGrids provides global gridded soil properties at 250 m native support, including texture fractions, and its version 2.0 products document the global modeling framework (Hengl *et al*., 2017; Poggio *et al*., 2021) [10, 20].

The ward layer contains 107 unique GRID3 ward features. After intersection with the watershed footprint, the analysis summarizes the Anambra, Delta, and Enugu portions represented in the study polygon. Hydrographic layers provide the river-distance and drainage-density factors, while HAND and TWI are represented by their respective input rasters.

**Table 2:** Raster grid properties before harmonization

| Factor | Rows × columns | Type | Cell (m) |
|---|---|---|---|
| Elevation | 2344 × 1617 | uint8 | 30.000000 |
| Slope | 2344 × 1617 | float32 | 30.000000 |
| HAND | 2344 × 1617 | float32 | 30.000000 |
| River distance | 2336 × 1606 | float32 | 30.000000 |
| Drainage Density | 2335 × 1604 | float32 | 30.000000 |
| TWI | 2271 × 1561 | float32 | 30.860780 |
| Rainfall | 2515 × 1781 | int16 | 30.000000 |
| Clay | 2335 × 1604 | float32 | 30.000000 |

All raster inputs are single-band GeoTIFFs in EPSG:32632. Bounds are outer pixel edges. The elevation grid defines the 30 m analysis grid used to align the continuous factor surfaces.

### 2.3. Spatial Harmonization and Treatment of Missing Cells

All raster layers were aligned in WGS 84 / UTM Zone 32N (EPSG:32632), a metric projected coordinate system appropriate for the study area. Elevation defined the snap grid, with 1,617 columns and 2,344 rows at 30 m cell spacing. Ward polygons were transformed from WGS 84 (EPSG:4326) to the analysis CRS and intersected with the watershed study polygon before area summaries were calculated.

Continuous factor rasters were resampled to the elevation grid using bilinear interpolation and clipped to the rasterized watershed footprint. The complete decision matrix contains 2,010,837 cells with valid values for all eight factors. This common analysis area provides the consistent spatial support for normalization, LOPCOW weighting, index calculation, and class-area summaries.

The complete-factor footprint covers 1,809.7533 km², equivalent to 96.79296% of the rasterized watershed boundary. The remaining 66,625 boundary cells, covering 59.9625 km², are recorded as unmapped in the coverage summaries and are excluded from the susceptibility index and class-area denominator.

### 2.4. Factor Definitions and Response Directions

Table 3 defines the eight conditioning factors and the susceptibility direction used in normalization. Factors for which lower values indicate greater susceptibility were treated as cost criteria; factors for which higher values indicate greater susceptibility were treated as benefit criteria. This orientation places all normalized factor values on a common scale where larger values indicate greater susceptibility.

**Table 3:** Factor definitions and response directions

| Factor | Factor meaning / definition | Response direction and normalization |
|---|---|---|
| Elevation | Absolute terrain height. | Lower values → higher susceptibility; cost min–max normalization. |
| Slope | Terrain gradient, conventionally $\arctan(\sqrt{(p^2 + q^2)}) \times 180/\pi$. | Lower values → higher local retention; cost min–max normalization. |
| HAND | Vertical height above the drainage cell reached along a hydrological flow path. | Lower values → lower relative height above drainage; cost min–max normalization. |
| River distance | Planar distance to the Anambra River and major tributaries. | Lower values → greater proximity to potential river overflow; cost min–max normalization. |
| Drainage density | Channel length per neighborhood area. | Higher values → greater drainage-path concentration; benefit min–max normalization. |
| TWI | $\ln(a / \tan \beta)$, where a is specific contributing area and β is slope in radians. | Higher values → greater topographic wetness tendency; benefit min–max normalization. |
| Rainfall | Spatial rainfall surface. | Higher values → greater water input; benefit min–max normalization. |
| Clay | Soil clay content, expressed as a percentage. | Higher values → greater potential for restricted matrix infiltration; benefit min–max normalization. |

Direction rationale is based on established flood-index and terrain-hydrology studies (Kazakis *et al*., 2015; Gigović *et al*., 2017; Nobre *et al*., 2011; Beven & Kirkby, 1979; Saxton & Rawls, 2006; Islam *et al*., 2025) [2, 8, 13, 14, 18, 21].

### 2.5. LOPCOW Weighting and Weighted Combination

LOPCOW weighting follows the formulation of Ecer and Pamucar (2022) [5]. The eight factor rasters were represented as a cell-by-factor decision matrix over the complete-factor footprint. Each criterion was normalized according to its response direction, distributional statistics were calculated across all eligible cells, and normalized weights were used in a weighted linear combination to generate the susceptibility index.

$$X = [x_{ij}], i = 1, \dots, m; j = 1, \dots, 8. \quad (1)$$

For each column, $a_j = \min_i(x_{ij})$ and $b_j = \max_i(x_{ij})$ were computed only over the complete common mask. Benefit criteria were transformed by Equation 2 and cost criteria by Equation 3. Thus r = 1 consistently denotes the more susceptible end of each observed factor range.

$$r_{ij} = (x_{ij} - a_j)/(b_j - a_j), for higher - is - more - susceptible factors. \quad (2)$$

$$r_{ij} = (b_j - x_{ij})/(b_j - a_j), for lower - is - more - susceptible factors. \quad (3)$$

Elevation, slope, HAND, and river distance were normalized as cost criteria; drainage density, TWI, rainfall, and clay were normalized as benefit criteria. Each factor had a nonzero range and standard deviation across the complete-factor footprint.

$$\mu_j = (1/m)\Sigma_i r_{ij}; \sigma_j = \sqrt{(1/m)\Sigma_i (r_{ij} - \mu_j)^2}. \quad (4)$$

$$RMS_j = \sqrt{(1/m)\Sigma_i r_{ij}^2}; PV_j = 100\left|ln(RMS_j/\sigma_j)\right|. \quad (5)$$

$$w_j = PV_j/\Sigma_k^{=18} PV_k; \Sigma_j^{=18} w_j = 1. \quad (6)$$

The population standard deviation was used because the matrix enumerates the full set of mapped cells. The logarithmic percentage value (PV) is computed from the ratio of the normalized root-mean-square value to the standard deviation. Each criterion weight is its PV divided by the sum of PV values across the eight criteria.

The normalized factors were combined additively using Equation 7 to produce a continuous flood-susceptibility index, with larger values representing greater relative susceptibility within the study area.

$$F_i = \Sigma_j^{=18} w_j r_{ij}. \quad (7)$$

Because $RMS_j^2 = \mu_j^2 + \sigma_j^2$, the LOPCOW measure can also be written as $PV_j = 50\ \ln[1 + (\mu_j/\sigma_j)^2]$ when $\sigma_j > 0$. The final weight therefore reflects both the normalized mean and dispersion of each criterion across the mapped cells.

### 2.6. Classification, Area Measurement, and Ward-Area Overlay

The continuous susceptibility index was divided into five equal-width intervals spanning its observed minimum and maximum. The class labels—very low, low, moderate, high, and very high—represent relative bands of the composite index. Cell counts were converted to area using the 30 m grid, and class percentages were calculated as a share of the complete-factor footprint.

$$A_k = N_k \times 30 \times 30 / 10^6\ km^2; \quad P_k = 100\ N_k / m. \quad (8)$$

Ward polygons were projected to EPSG:32632 and intersected with the watershed polygon. Each raster cell was assigned to the ward portion containing its center, and class areas and mapped coverage were summarized by ward. Two measures were calculated: the absolute area in high and very high classes and that area as a percentage of classified cells in each ward portion. Table 7 reports class intersections and dominant classes; Tables 8 and 9 provide ranked ward and state-level summaries.

### 2.7. Software and Reproducible Outputs

Spatial analysis used Python with NumPy, Rasterio/GDAL, GeoPandas, SciPy, Shapely, and Matplotlib. The processing sequence produced aligned factor rasters, LOPCOW calculations, a continuous index, five susceptibility classes, map figures, and ward-level area tables.

## 3. Results

### 3.1. Factor Distributions and Spatial Coverage

Table 4 summarizes the eight factors over the 2,010,837 complete-factor cells. Elevation ranges from 18 to 252 m, with a mean of 48.992 m and a median of 35 m. Mean slope is 2.088° and the median is 1.467°, indicating that low-gradient terrain occupies much of the mapped footprint. HAND has a mean of 18.308 m and a median of 6.987 m, while mean distance to a major river is 1,907.342 m. Rainfall values have a mean of 2,752.565 and clay content has a mean of 20.167.

**Table 4:** Descriptive statistics of the eight factors

| Factor | Minimum | Maximum | Mean | SD | Median |
|---|---|---|---|---|---|
| Elevation | 18.000 | 252.000 | 48.992 | 33.710 | 35.000 |
| Slope | 0.000 | 31.227 | 2.088 | 2.256 | 1.467 |
| HAND | 0.000 | 228.970 | 18.308 | 25.301 | 6.987 |
| Distance to river | 0.000 | 10621.342 | 1907.342 | 1882.557 | 1297.998 |
| Drainage density | 0.000 | 1.487 | 0.358 | 0.303 | 0.338 |
| TWI | 6.362 | 27.658 | 13.756 | 1.935 | 13.785 |
| Rainfall | 2370.000 | 2967.000 | 2752.565 | 106.322 | 2753.000 |
| Clay | 11.958 | 28.840 | 20.167 | 1.913 | 20.092 |

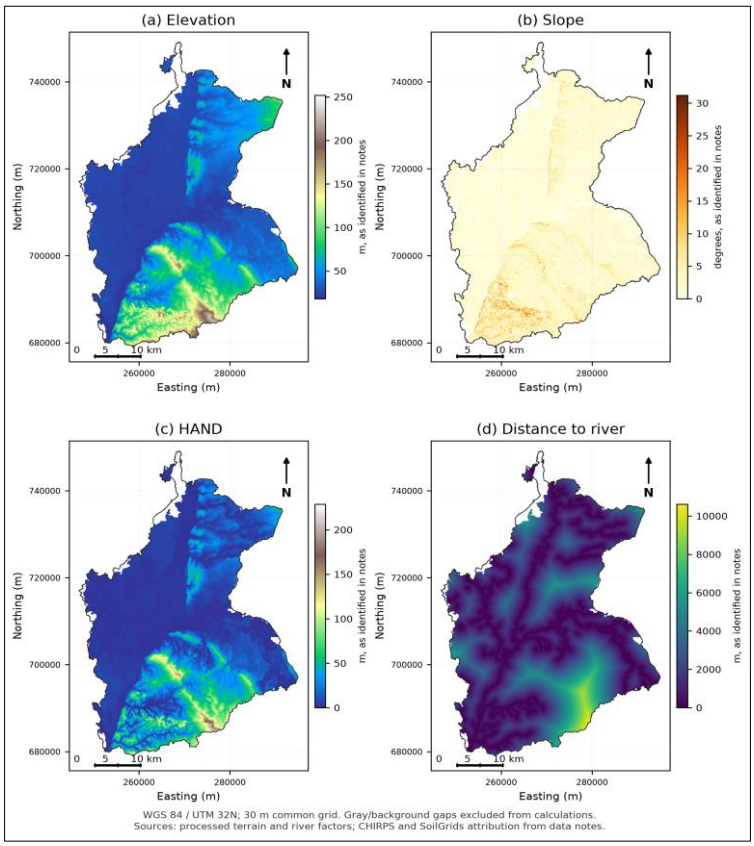



**Fig 1:** Terrain and proximity factors on the analysis grid: (a) elevation, (b) slope, (c) HAND, and (d) distance to the Anambra River and major tributaries.

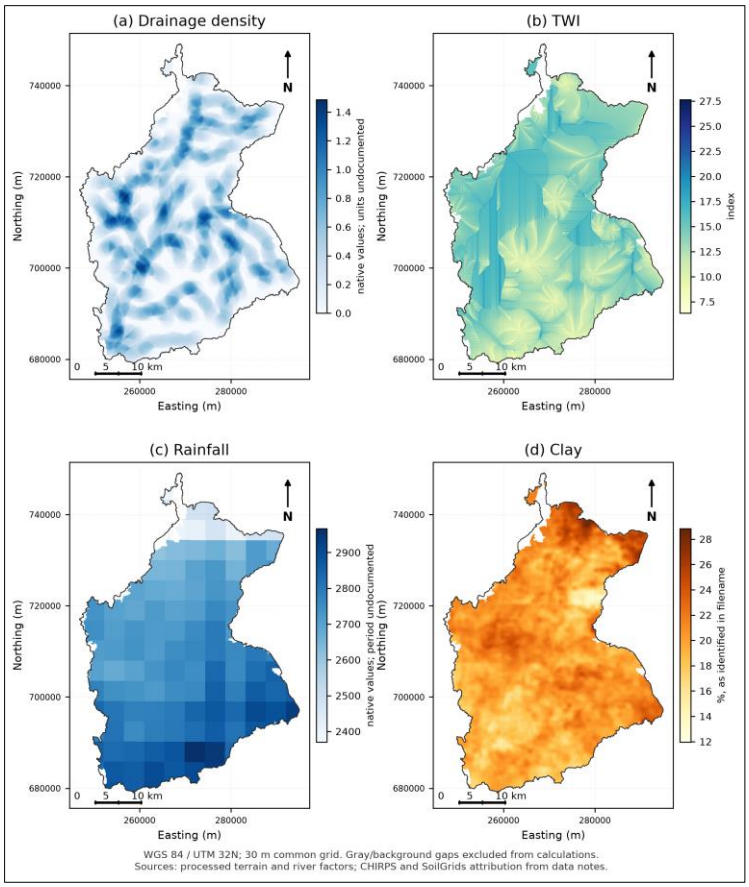



**Fig 2:** Hydrographic, wetness, rainfall, and soil factors: (a) drainage density, (b) TWI, (c) rainfall, and (d) clay content. Panels are aligned to the common analysis grid.

Elevation, HAND, and river distance are expressed in metres; slope is in degrees and clay in percent. Rainfall and drainage density retain the numerical scales of their input rasters. Descriptive statistics use the common complete-factor cells.

The factor maps show a broad low-relief western and northern tract and higher terrain toward the south-central and southeastern parts of the study area (Figure 1a–c). River-distance values increase away from the Anambra River and its major tributaries (Figure 1d). The mapped terrain and proximity patterns provide the spatial context for the factor statistics in Table 4.

Drainage-density values range from 0 to 1.4875, with a mean of 0.3580, and form localized concentrations along drainage corridors (Figure 2a). TWI ranges from 6.362 to 27.658, with a mean of 13.756 and a median of 13.785 (Figure 2b). Rainfall has a mean of 2,752.565, while clay content ranges from 11.958% to 28.840% (Figure 2c–d). These spatial distributions show how the hydrological, climatic, and soil criteria complement the terrain factors.

### 3.2. LOPCOW Intermediate Quantities and Factor Weights

Table 5 presents the normalized means, standard deviations, root-mean-square values, PV measures, and final LOPCOW weights. Slope has the highest PV (256.130) and weight (0.202264), followed by HAND (0.167934) and elevation (0.142859). The three terrain criteria together account for 51.31% of total weight. Drainage density has the smallest weight (0.034512), while river distance, clay, TWI, and rainfall contribute 12.28%, 11.71%, 10.85%, and 10.41%, respectively.

**Table 5:** LOPCOW calculations and final criterion weights

| Factor | μ | σ | RMS | PV | Weight | % |
|---|---|---|---|---|---|---|
| Elevation | 0.867555 | 0.144060 | 0.879435 | 180.905 | 0.142859 | 14.29 |
| Slope | 0.933133 | 0.072258 | 0.935927 | 256.130 | 0.202264 | 20.23 |
| HAND | 0.920043 | 0.110499 | 0.926654 | 212.657 | 0.167934 | 16.79 |
| Distance to river | 0.820424 | 0.177243 | 0.839351 | 155.511 | 0.122806 | 12.28 |
| Drainage density | 0.240657 | 0.203640 | 0.315254 | 43.702 | 0.034512 | 3.45 |
| TWI | 0.347188 | 0.090881 | 0.358886 | 137.345 | 0.108461 | 10.85 |
| Rainfall | 0.640812 | 0.178094 | 0.665099 | 131.762 | 0.104052 | 10.41 |
| Clay | 0.486268 | 0.113318 | 0.499297 | 148.300 | 0.117112 | 11.71 |

Slope's normalized mean is 0.933133 and its normalized standard deviation is 0.072258, yielding the largest PV and weight. HAND and elevation also have high normalized means (0.920043 and 0.867555) and substantial weights. The drainage-density weight reflects its normalized mean of 0.240657 and standard deviation of 0.203640. Figure 3 presents the relative weighting of all eight factors.

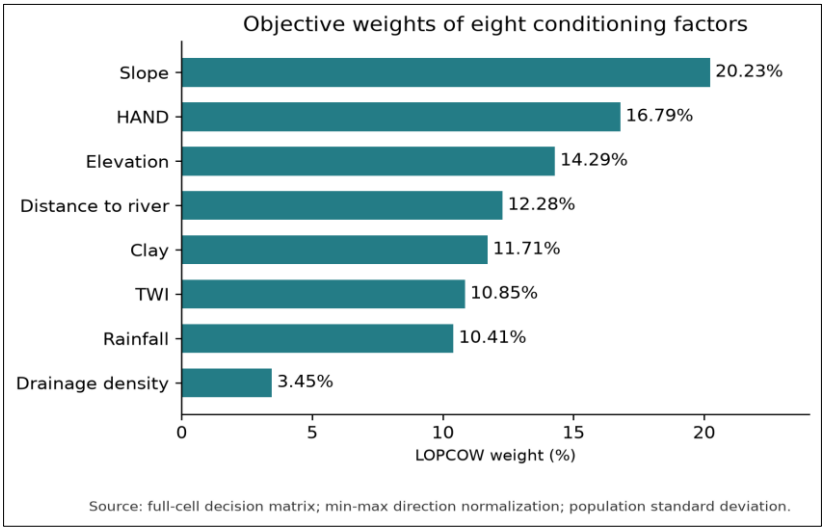



**Fig 3:** LOPCOW weights for the eight flood-conditioning factors, calculated from direction-normalized raster-cell values. Bars are ordered by weight; values are shown as percentages.

### 6.3. Susceptibility Index and Class Areas

The continuous susceptibility index ranges from 0.298647 to 0.890720, with a mean of 0.737525, median of 0.753121, and population standard deviation of 0.064465. Table 6 lists the class thresholds, cell counts, mapped areas, and percentages. High susceptibility covers 974.1528 km² (53.83%), and very high susceptibility covers 644.1579 km² (35.59%). Together, these classes occupy 1,618.3107 km², or 89.42% of the complete-factor area.

**Table 6:** Susceptibility class thresholds, cell counts, areas, and percentages

| Class | Index interval | Cells | Area (km²) | Mapped area (%) |
|---|---|---|---|---|
| Very low | 0.298647433 to 0.417061972 | 1,543 | 1.3887 | 0.0767 |
| Low | 0.417061972 to 0.535476510 | 18,028 | 16.2252 | 0.8965 |
| Moderate | 0.535476510 to 0.653891049 | 193,143 | 173.8287 | 9.6051 |
| High | 0.653891049 to 0.772305587 | 1,082,392 | 974.1528 | 53.8279 |
| Very high | 0.772305587 to 0.890720126 | 715,731 | 644.1579 | 35.5937 |
| Total mapped | | 2,010,837 | 1809.7533 | 100.0000 |

Lower class limits are inclusive and upper limits are exclusive, except for the final maximum. Classification used unrounded cutoffs. Percentages use the 1,809.7533 km² complete-factor footprint.

High and very high susceptibility occupy broad areas of the low-relief western and northern sectors, while moderate and lower classes occur more frequently in the higher southern interior (Figure 4). This pattern is consistent with the factor distributions in Figures 1 and 2 and the dominant weights assigned to slope, HAND, and elevation.

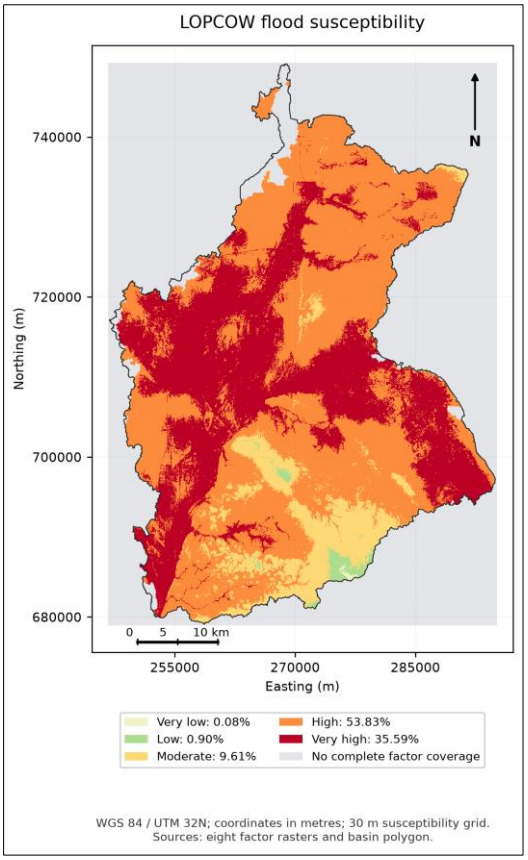



**Fig 4:** Flood-susceptibility classes produced from five equal intervals of the observed LOPCOW index. The mapped cells cover 1,809.7533 km² of the watershed footprint.

Class-conditioned means quantify this spatial contrast. The very high class has mean elevation of 27.596 m, slope of 0.959°, HAND of 2.802 m, river distance of 844.742 m, and TWI of 14.946. In the very low class, mean elevation is 216.467 m, slope 7.192°, HAND 192.722 m, river distance 8,474.806 m, and TWI 10.415. Mean clay content increases from 17.571% in the very low class to 20.658% in the very high class, while mean rainfall is 2,940.028 and 2,757.893, respectively.

### 6.4. Ward-Area Exposure

The ward overlay comprises 107 watershed-clipped ward portions, of which 103 contain classified cells. Ninety-three portions contain some high or very high susceptibility, and 76 of the 103 mapped portions have at least half of their classified area in those categories. Table 7 reports class intersections and dominant classes; Figures 5 and 6 show the ward geography and the high-plus-very-high proportion by ward.

Ward counts are nonexclusive because one ward portion can intersect several susceptibility classes. Dominant class is the category with the largest mapped area. The four portions without classified cells are identified in the ward summaries.

**Table 7:** Ward intersections and dominant susceptibility classes

| Class | Area (km²) | Wards containing class | Wards dominated by class |
|---|---|---|---|
| Very low | 1.3887 | 4 | 0 |
| Low | 16.2252 | 34 | 4 |
| Moderate | 173.8287 | 76 | 23 |
| High | 974.1528 | 91 | 53 |
| Very high | 644.1579 | 68 | 23 |
| Unmapped area | 59.9625 | 55 with unmapped cells | 4 entirely unmapped |

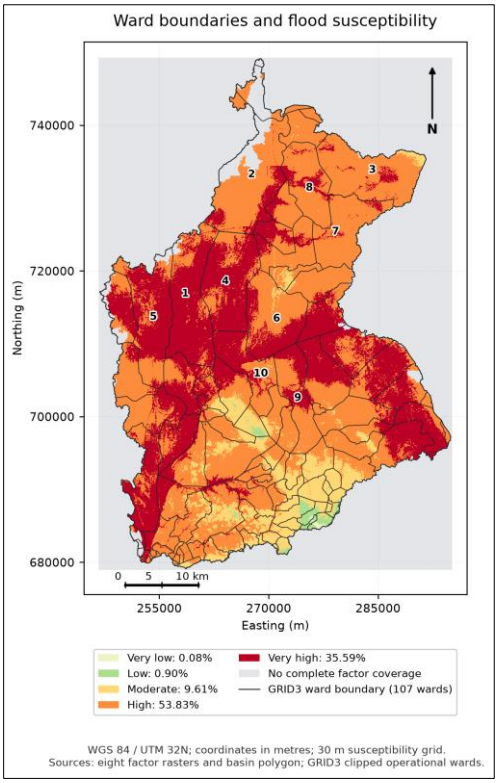



**Fig 5:** GRID3 ward portions overlaid on the flood-susceptibility classes within the watershed study area. All 107 unique ward portions are shown.

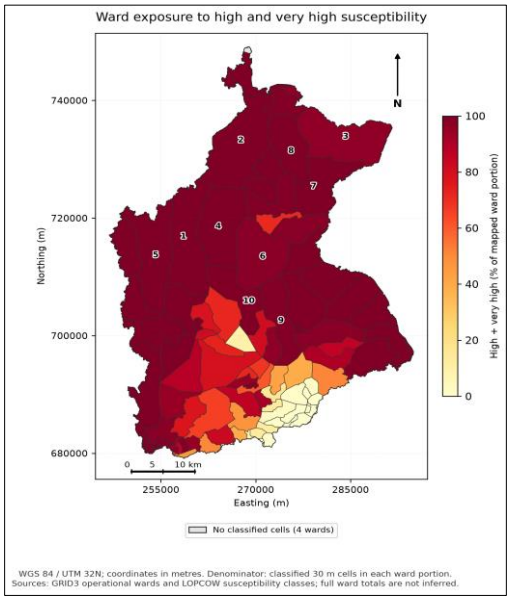



**Fig 6:** High-plus-very-high susceptibility as a percentage of classified area in each watershed-clipped ward portion. Gray indicates portions without classified cells.

High or very high susceptibility occurs in 93 ward portions. In 76 of the 103 mapped portions (73.79%), these classes together cover at least 50% of classified area. Table 8 ranks the ten portions with the largest high-plus-very-high areas, led by Abegbu / Iyiora (91.3635 km²), Enugu-Otu (91.2870 km²), and Omasi (88.0389 km²).

Ward portions are ranked by combined high and very high area. Susceptibility percentages use classified cells in each portion, and mapped-coverage percentages use all rasterized boundary cells assigned to the portion. Table 8 lists the ten highest values.

Table 9 summarizes the state-labelled portions of the watershed. Anambra portions contain 1,800.9045 km² of classified cells, including 1,609.4628 km² in high and very high classes. Delta portions contribute 1.7766 km² of classified area, and Enugu portions contribute 7.0722 km², including 7.0713 km² in the two highest classes.

**Table 8:** Ten ward portions with the largest high-plus-very-high susceptibility area

| Rank | Ward code | Ward name | LGA | High + very high (km²) | High + very high (%) | Mapped coverage (%) |
|---|---|---|---|---|---|---|
| 1 | ANSNZM01 | Abegbu / Iyiora | Anambra West | 91.3635 | 100.00 | 97.92 |
| 2 | ANSAAH03 | Enugu-Otu | Anambra East | 91.2870 | 99.78 | 82.43 |
| 3 | ANSNKK05 | Omasi | Ayamelum | 88.0389 | 96.20 | 98.30 |
| 4 | ANSAAH04 | Eziagulu Otu | Anambra East | 82.5057 | 100.00 | 100.00 |
| 5 | ANSNZM03 | Mmiata | Anambra West | 80.5896 | 100.00 | 96.29 |
| 6 | ANSNKK01 | Anaku | Ayamelum | 71.8551 | 97.73 | 100.00 |
| 7 | ANSNKK11 | Umumbo | Ayamelum | 60.4161 | 99.99 | 99.01 |
| 8 | ANSNKK03 | Ifite-O 2 | Ayamelum | 53.0649 | 99.87 | 100.00 |
| 9 | ANSAAH05 | Igbariam | Anambra East | 47.9997 | 99.10 | 100.00 |
| 10 | ANSAAH07 | Nando 2 | Anambra East | 47.0511 | 99.37 | 100.00 |

**Table 9:** Ward portions and exposure grouped by state attribute

| State | Wards | Polygon area (km²) | Mapped area (km²) | Unmapped area (km²) | High + very high (km²) |
|---|---|---|---|---|---|
| Anambra | 101 | 1843.5687 | 1800.9045 | 42.6861 | 1609.4628 |
| Delta | 3 | 4.8930 | 1.7766 | 3.1176 | 1.7766 |
| Enugu | 3 | 21.2307 | 7.0722 | 14.1588 | 7.0713 |

## 4. Discussion of Results

### 4.1. Hydrological Interpretation of the Mapped Pattern

The highest susceptibility class occurs in low terrain both in absolute elevation and relative height above drainage. Its mean HAND of 2.802 m and mean river distance of 844.742 m characterize locations near channel level and close to major rivers. These settings provide direct pathways for overbank flow and surface-water accumulation, consistent with the hydrological interpretation of HAND and river proximity in flood mapping (Nobre *et al*., 2011; Kazakis *et al*., 2015) [14, 18].

HAND complements absolute elevation by describing vertical position relative to the drainage network. In the study area, mean HAND falls from 192.722 m in the very low class to 2.802 m in the very high class, clearly separating upland positions from drainage-connected lowlands. The joint pattern of low elevation, gentle slope, and short river distance concentrates the highest index values along floodplain and river-corridor terrain.

Rainfall and terrain display distinct spatial gradients across the watershed. Higher rainfall values occur toward the south, while high susceptibility is most extensive across low-relief sectors, where elevation, slope, HAND, and river proximity jointly favor water accumulation. The class-conditioned means—2,940.028 in the very low class and 2,757.893 in the very high class—show that the composite pattern reflects the weighted interaction of all eight criteria rather than rainfall alone.

Clay contributes 11.71% of the LOPCOW weight and its mean increases from 17.571% in the very low class to 20.658% in the very high class. This pattern is consistent with the role of finer soil texture in reducing matrix infiltration potential, while soil structure and organic matter also influence hydraulic behavior (Saxton & Rawls, 2006) [21]. The clay layer therefore adds a meaningful soil-property dimension to the terrain and hydrological factors.

### 4.2. What the LOPCOW Weights and Class Proportions Mean

Slope receives the largest coefficient because its normalized values have a high mean relative to their dispersion across mapped cells. HAND and elevation also receive high weights and normalized means, creating a strong contribution from lowland terrain conditions. Drainage density receives a smaller coefficient because its normalized distribution has a lower mean and comparatively larger spread. These weights describe the contribution of each oriented raster distribution within the LOPCOW calculation.

The weighted sum retains high memberships for lowland factors across much of the footprint. Mean normalized memberships are 0.933133 for slope, 0.920043 for HAND, and 0.867555 for elevation. Their combined weight is 51.31%, and the five-class map places 89.42% of complete-factor area in the high and very high categories. This concentration defines the spatial prioritization pattern of the selected eight-factor model.

The mapped pattern complements flood studies elsewhere in Anambra and Nigeria. Northern Anambra and Ayamelum assessments have used different criteria and weighting strategies, while the lower Niger study around Onitsha and recent Nigerian assessments apply distinct factor sets and spatial methods (Igboanugo *et al*., 2023; Chinedu *et al*., 2024; Okeke & Ekemezie, 2026; Isioye *et al*., 2026; Montien Tique *et al*., 2026) [3, 11, 12, 17, 19]. The present analysis adds a watershed-scale LOPCOW assessment with explicit cell-level weights, index thresholds, and ward-area summaries.

### 4.3. Implications for Ward-Level Planning

The ward overlay identifies where the largest mapped high-plus-very-high areas occur. Abegbu / Iyiora, Enugu-Otu, Omasi, Eziagulu Otu, and Mmiata lead the ranked list of ward portions. These results support prioritization of drainage appraisal, floodplain development review, and local preparedness activities in the areas with the greatest mapped extent. Area and percentage summaries provide complementary measures of the size and concentration of susceptibility within each portion.

Absolute high-plus-very-high area highlights the portions with the largest spatial extent, while the within-portion percentage shows how much classified area falls in the two highest classes. Seventy-six mapped portions have at least half their classified area in high or very high susceptibility. Umudei / Inland Town 1, Ojjor, Olo 2, and Abagana 4 contain no classified cells in the common analysis mask. The full ward inventory in Table 8 and the corresponding exposure summary identify each portion and its mapped area.

## 5. Conclusion

The LOPCOW integration of eight conditioning factors produced a continuous flood-susceptibility index for 1,809.7533 km² of the Anambra River watershed. Slope received the largest objective weight (20.23%), followed by HAND (16.79%) and elevation (14.29%). Together, these terrain criteria contribute 51.31% of the total weight and define the model's strong emphasis on low-relief, drainage-connected locations.

The index ranged from 0.298647 to 0.890720. Equal-width classification placed 974.1528 km² in the high class and 644.1579 km² in the very high class, together accounting for 89.42% of mapped area. The very high class is characterized by low mean elevation (27.596 m), low mean HAND (2.802 m), and gentle mean slope (0.959°). These quantitative patterns show that susceptibility is concentrated in low-lying terrain near the drainage network.

The ward summaries translate the continuous watershed map into locally interpretable priorities. Of 107 ward portions, 103 contain classified cells, 93 intersect high or very high susceptibility, and 76 have at least half of classified area in these classes. Abegbu / Iyiora, Enugu-Otu, and Omasi have the largest high-plus-very-high areas. The factor maps, weighting results, susceptibility zones, and ward summaries together provide a clear basis for targeted floodplain planning, drainage assessment, and preparedness across the Anambra River corridor.

## References


1. Anambra State Government. About Anambra, from. [date unknown]. Available from: https://anambrastate.gov.ng/about-anambra/ [cited November 1, 2026]
2. Beven KJ, Kirkby MJ. A physically based, variable contributing area model of basin hydrology. Hydrological Sciences Bulletin. 1979;24(1):43-69. doi:10.1080/02626667909491834
3. Chinedu AD, Ezebube NM, Uchegbu S, Ozorme VA. Integrated assessment of flood susceptibility and exposure rate in the lower Niger Basin, Onitsha, Southeastern Nigeria. Frontiers in Earth Science. 2024;12:1394256. doi:10.3389/feart.2024.1394256
4. Climate Hazards Center. CHIRPS: Rainfall estimates from rain gauge and satellite observations. [date unknown]. Available from: https://chc.ucsb.edu/data/chirps
5. Ecer F, Pamucar D. A novel LOPCOW-DOBI multi-criteria sustainability performance assessment methodology: An application in developing country banking sector. Omega. 2022;112:102690. doi:10.1016/j.omega.2022.102690
6. Farr TG, Rosen PA, Caro E, Crippen R, Duren R, Hensley S, *et al*. The Shuttle Radar Topography Mission. Reviews of Geophysics. 2007;45(2):RG2004. doi:10.1029/2005RG000183
7. Funk C, Peterson P, Landsfeld M, Pedreros D, Verdin J, Shukla S, *et al*. The climate hazards infrared precipitation with stations—a new environmental record for monitoring extremes. Scientific Data. 2015;2:150066. doi:10.1038/sdata.2015.66
8. Gigović L, Pamučar D, Bajić Z, Drobnjak S. Application of GIS-interval rough AHP methodology for flood hazard mapping in urban areas. Water. 2017;9(6):360. doi:10.3390/w9060360
9. GRID3. Geospatial data Nigeria, from. [date unknown]. Available from: https://grid3.org/geospatial-data-nigeria [cited November 1, 2026]
10. Hengl T, Mendes de Jesus J, Heuvelink GBM, Ruiperez Gonzalez M, Kilibarda M, Blagotić A, *et al*. SoilGrids250m: Global gridded soil information based on machine learning. PLOS ONE. 2017;12(2):e0169748. doi:10.1371/journal.pone.0169748
11. Igboanugo IR, Iheukwumere SO, Obikwelu MC, Ozoemene ML, Umeogu CC, Eburu PI, *et al*. Analysis of flood susceptibility in northern Anambra State: A GIS multi-criteria decision making model of AHP, BWM. and CRITIC method. International Journal of Applied Science and Engineering Review. 2023;4(4):106-133. doi:10.52267/IJASER.2023.4408
12. Isioye O, Zailani MM, Hassan M, Gaya IF, Abubakar ML. Flood susceptibility assessment using GIS and an analytical hierarchy process in Ilorin Metropolis, Kwara, Nigeria. Discover Cities. 2026;3:197. doi:10.1007/s44327-026-00380-3
13. Islam T, Zeleke EB, Afroz M, Melesse AM. A systematic review of urban flood susceptibility mapping: Remote sensing, machine learning, and other modeling approaches. Remote Sensing. 2025;17(3):524. doi:10.3390/rs17030524
14. Kazakis N, Kougias I, Patsialis T. Assessment of flood hazard areas at a regional scale using an index-based approach and analytical hierarchy process: Application in Rhodope–Evros region, Greece. Science of the Total Environment. 2015;538:555-563. doi:10.1016/j.scitotenv.2015.08.055
15. Lehner B, Verdin K, Jarvis A. New global hydrography derived from spaceborne elevation data. Eos, Transactions American Geophysical Union. 2008;89(10):93-94. doi:10.1029/2008EO100001
16. Malczewski J. GIS-based multicriteria decision analysis: A survey of the literature. International Journal of Geographical Information Science. 2006;20(7):703-726. doi:10.1080/13658810600661508
17. Montien Tique WF, Sapena M, Weigand M, Groth S, Geiß C, Taubenböck H. A comparative assessment of data-driven flood susceptibility mapping in Nigeria.

Natural Hazards. 2026;122:139. doi:10.1007/s11069-025-07868-y
18. Nobre AD, Cuartas LA, Hodnett M, Rennó CD, Rodrigues G, Silveira A, *et al*. Height above the nearest drainage—a hydrologically relevant new terrain model. Journal of Hydrology. 2011;404(1–2):13-29. doi:10.1016/j.jhydrol.2011.03.051
19. Okeke UC, Ekemezie EJ. Geospatial analysis of flood drivers and flood risk in Ayamelum Local Government Area, Anambra State, Nigeria. Journal of Spatial Information Sciences. 2026;3(1):201-224. Available from: https://journals.unizik.edu.ng/jsis/article/view/8304
20. Poggio L, de Sousa LM, Batjes NH, Heuvelink GBM, Kempen B, Ribeiro E, *et al*. SoilGrids 2.0: Producing soil information for the globe with quantified spatial uncertainty. SOIL. 2021;7(1):217-240. doi:10.5194/soil-7-217-2021
21. Saxton KE, Rawls WJ. Soil water characteristic estimates by texture and organic matter for hydrologic solutions. Soil Science Society of America Journal. 2006;70(5):1569-1578. doi:10.2136/sssaj2005.0117
22. Sen S, Das J. Geospatial AI for flood susceptibility mapping: A systematic literature review of parameters, methods, uncertainty quantification, and resilience frameworks. Frontiers in Environmental Science. 2026;14:1896243. doi:10.3389/fenvs.2026.1896243
23. Sørensen R, Zinko U, Seibert J. On the calculation of the topographic wetness index: Evaluation of different methods based on field observations. Hydrology and Earth System Sciences. 2006;10(1):101-112. doi:10.5194/hess-10-101-2006
24. Geological Survey US. USGS EROS archive—Digital elevation—Shuttle Radar Topography Mission (SRTM) 1 arc-second global. 2018. Available from: https://www.usgs.gov/centers/eros/science/usgs-eros-archive-digital-elevation-shuttle-radar-topography-mission-srtm-1

**How to Cite This Article**

Okafor, O.C, Ono, M.N, Emengini, E.J, *et al*. Flood susceptibility assessment in the Anambra river watershed using the LOPCOW weighting technique. Int J Future Eng Innov. 2026;3(6):65-75.

**Creative Commons (CC) License**

This is an open access journal, and articles are distributed under the terms of the Creative Commons Attribution NonCommercial-ShareAlike 4.0 International (CC BY-NC-SA 4.0) License, which allows others to remix, tweak, and build upon the work non-commercially, as long as appropriate credit is given and the new creations are licensed under the identical terms